

# Impact of Morphological Parameters on the Elastic Properties of Composite Hydrogen Pipe

Benchaou Masouda<sup>1</sup>, Hermama Chaïmaâ<sup>1</sup>, Touaiher Imane<sup>1</sup>, El Asri Hamid<sup>2</sup>, Moubachir Younes<sup>1</sup> and Taibi Saoudi<sup>1</sup>

<sup>1</sup> Quality, safety and maintenance research team Université Mohammed V de Rabat, EMI, Rabat, Morocco

<sup>2</sup> Principal Piping Engineer at JESA, Morocco, [masouda.benchaou@research.emi.ac.ma](mailto:masouda.benchaou@research.emi.ac.ma)

**Abstract.** Advanced composite materials are increasingly used in hydrogen gas transport pipelines due to their excellent mechanical resistance, good corrosion resistance with lower density compared to steel material. The morphological properties the key parameters that gueven the mechanical behaviors of composite. The objectif of study is to incestynte the property-structure relationship using ANSYS Material Design, considering various morphological effects such as fiber fraction, fiber diameter, fiber distribution, and fiber material type. The analysis showed that the mechanical properties of the unidirectional composite are significantly affected by morphological parameters. In fact, smaller fiber diameters and higher volume fractions improve orthogonal stiffness and overall strength. Moreover The study discuss The effect of anisotropy variation of elastic properties for carbon-fiber reinforced polymers (CFRP) and glass-fiber reinforced polymers (GFRP). Specifically, CFRP composites exhibit a pronounced increase in the anisotropy with fiber volume fraction, reflecting their highly directional stiffnes. In contrast, GFRP composites show a decrease in this ratio as fiber volume fraction increases

**Keywords:** Composite Pipelines, Morphological parameters, Hydrogen Transport, Finite Element Analysis, Numerical homogenization

## 1 INTRODUCTION

The safe and efficient transport of hydrogen over long and short distances remains a major challenge in the development of hydrogen infrastructure. Stainless steel pipelines, despite their widespread use, face critical limitations when exposed to hydrogen, primarily due to the phenomenon of hydrogen embrittlement [1]. This degradation leads

to crack formation, material failure, and reduced durability, requiring frequent maintenance and increasing operational cost. Although the high density of the metallic pipe [2], increases considerably the cost of the pipe rack.

As a response to these limitations, composite materials have emerged as a promising alternative. Composites, particularly fiber-reinforced polymer (FRP), offer several advantages over stainless steel, including higher corrosion resistance, lower susceptibility to hydrogen embrittlement, and reduced weight and cost [3-5].

Previous studies have primarily focused on the corrosion resistance and structural performance of composites in hydrogen environments. Limited research has explored the full range of mechanical properties and key factors such as fiber diameter, fiber distribution, and fiber volume fraction on the strength and durability of composite pipelines. Additionally, More works are needed to compare composite and to stainless steel pipelines under the same operational conditions [6,7]. This study primarily aims to perform a numerical analysis of unidirectional composite pipelines made from E-glass with a vinyl-ester resin matrix, using ANSYS Material Design. We focus on key parameters such as fiber type, fiber diameter, fiber fraction and fiber distribution evaluate the material properties.

## 2 Homogenization Theory

Homogenization theory is widely used to estimate the effective mechanical properties of heterogeneous materials like fiber-reinforced composites, bridging the microscale morphology (fiber and matrix) with the macroscopic mechanical response. Two main approaches exist: asymptotic homogenization, a mathematically rigorous method based on periodic unit cells and scale separation, which employs asymptotic expansions to derive the homogenized elasticity tensor—often solved numerically using the Finite Element Method (AHM-FEM); and statistical or mean-field models, which consider average interactions between inclusions and matrix but typically neglect direct interactions between neighboring inclusions. For periodic or highly structured composites, more refined cluster-based methods, such as the modified tangent cluster model, improve prediction accuracy by accounting for local interactions and anisotropy effects due to the spatial arrangement of inclusions.[8-9]

Homogenization aims to determine the effective elastic properties of unidirectional composite materials by replacing the heterogeneous microstructure with an equivalent homogeneous material. Using Ansys Material Designer, a Representative Volume Element (RVE) is loaded under six cases: three uniaxial strains and three shear strains. The average stresses are used to construct the global stiffness matrix  $[D]$ , then inverted to get the compliance matrix  $[C]=[D]^{-1}$ , from which the following properties are extracted:

- Young's moduli:  $E_{11}, E_{22}, E_{33}$
- Shear moduli:  $G_{12}, G_{23}$ ,
- Poisson's ratios:  $\nu_{12}, \nu_{23}, \nu_{13}$

The 3D orthotropic stiffness matrix [D] can be expressed as:

$$\begin{bmatrix} \sigma_{11} \\ \sigma_{22} \\ \sigma_{33} \\ \sigma_{23} \\ \sigma_{13} \\ \sigma_{12} \end{bmatrix} = \begin{bmatrix} Q_{11} & Q_{22} & Q_{13} & 0 & 0 & 0 \\ Q_{12} & Q_{22} & Q_{23} & 0 & 0 & 0 \\ Q_{13} & Q_{23} & Q_{33} & 0 & 0 & 0 \\ 0 & 0 & 0 & Q_{44} & 0 & 0 \\ 0 & 0 & 0 & 0 & Q_{55} & 0 \\ 0 & 0 & 0 & 0 & 0 & Q_{66} \end{bmatrix} \begin{bmatrix} \varepsilon_x \\ \varepsilon_y \\ \varepsilon_z \\ \gamma_{xy} \\ \gamma_{yz} \\ \gamma_{zx} \end{bmatrix} \quad (1)$$

In this expression, Q11,Q22,Q33 represent the stiffness in the principal directions, Q12,Q13,Q23 are coupling terms due to Poisson effects, and Q44,Q55,Q66 correspond to shear moduli.[19] The Compliance Matrix [C] in the 3D orthotropic case has the following structure:

$$[C] = \begin{bmatrix} 1/E_1 & -\nu_{21}/E_2 & -\nu_{31}/E_3 & 0 & 0 & 0 \\ -\nu_{12}/E_1 & 1/E_2 & -\nu_{32}/E_3 & 0 & 0 & 0 \\ -\nu_{13}/E_1 & -\nu_{23}/E_2 & 1/E_3 & 0 & 0 & 0 \\ 0 & 0 & 0 & 1/G_{12} & 0 & 0 \\ 0 & 0 & 0 & 0 & 1/G_{23} & 0 \\ 0 & 0 & 0 & 0 & 0 & 1/G_{13} \end{bmatrix} \quad (2)$$

- Young's moduli: E11,E22,E33
- Shear moduli: G12,G23,G13
- Poisson's ratios:  $\nu_{12}, \nu_{23}, \nu_{13}$

### 3 Analytical Models for Elastic Properties

To complement the numerical analysis performed using ANSYS Material Designer, several analytical micromechanical models are considered to predict the effective elastic properties of unidirectional fiber-reinforced composites. These models are used in the literature and allow for estimating the mechanical response based on the properties and morphology of the constituent materials.

#### 3.1 Rule of Mixtures

The Rule of Mixtures provides a first-order approximation of the composite's effective modulus in the fiber direction (longitudinal modulus E11 and in the transverse direction E22 using the Voigt (isostrain) and Reuss (isostress) assumptions:

$$E_{11} = V_f E_f + V_m E_m \quad (3)$$

$$\frac{1}{E_{22}} = \frac{V_f}{E_f} + \frac{V_m}{E_m} \quad (4)$$

This approach is simple but assumes perfect alignment and no interaction effects. [14]

where:

- $E_{11}$  and  $E_{22}$  are the longitudinal and transverse Young's moduli of the composite.
- $V_f$  and  $V_m$  are the volume fractions of the fibers and matrix, respectively.
- $E_f$  and  $E_m$  are the Young's moduli of the fibers and matrix.

## 4 Materials and methods

An accurate selection of fiber and matrix materials is crucial for ensuring good mechanical performance of the composite pipeline. In this section, we present the elastic properties of the materials mostly used fiber or matrix in hydrogen transport applications. These properties are essential for calculating the unidirectional properties of the resulting composite material.

### 4.1 Elastic properties of fiber:

We assume that the mechanical properties of carbon fibers are orthotropic and glass fibers are isotropic [10,11], the table 1 present the properties of the different fibers according to Granta Ansys . Although E-glass fibers have lower tensile strength than S glass fibers [12], they offer a good balance between strength and cost, making them ideal for large-scale applications. On the other hand, carbon fibers exhibit significantly higher stiffness and strength compared to glass fibers, along with lower density and excellent fatigue resistance. These properties make them ideal for high-performance applications.

**Table 1.** Mechanical Properties of fibers

Fiber material	Elastic modulus (GPa)		Shear stress (GPa)		Poisson's ratio	
	E11	E22	G12	G23	$\nu_{11}$	$\nu_{22}$
<b>E-glass</b>	73			30		0,22
<b>S-glass</b>	90			37		0,22
<b>Carbon (230)</b>	230	23	9	8,21	0,2	0,4

### 4.2 Elastic properties of matrix:

The key criteria for resin selection include mechanical properties, resistance to chemical degradation, and suitability for long-term operational stability.

The matrix material must provide optimal durability, resistance to environmental factors, especially exposure to gaseous hydrogen, and efficient load transfer between fibers. In this regard, vinyl-ester resin offers superior chemical resistance and excellent adhesion to fibers compared to polyester and epoxy resins [13]. Furthermore, its high resistance to freeze-thaw cycles and humid conditions makes it particularly well-suited for infrastructure exposed to harsh environments, such as pressurized hydrogen transport [14].

Hydrogen can embrittle certain polymers through diffusion and chemical interactions with the matrix, making it essential to select a resin that offers better impermeability and mechanical resistance. The molecular structure of vinyl-ester ensures better tolerance to mechanical stress, reducing the risk of delamination and cracking [10,14]. Compared to epoxy and polyester resins, vinyl-ester offers an ideal balance between cost and performance, making it a suitable material for pipelines exposed to hydrogen gas transport under pressure.

In table 2, we present the elastic properties of matrix, assuming that they are isotropic.

**Table 2.** Mechanical Properties of Matrix Materials

<b>Matrix material</b>	<b>Elastic modulus (GPa)</b>	<b>Poisson's ratio</b>
<b>Vinyl-ester</b>	2.6 to 3.4	0,35
<b>Epoxy</b>	4.1	0,4
<b>Polyester</b>	3.45	0.39

### 4.3 Properties of morphological parameters of unidirectional composite:

The unidirectional properties of the composite material reflect the characteristics of a single ply in a laminated composite. In this section, we consider the reference material, which consists of laminated E-glass fibers embedded in a vinyl-ester resin matrix, produced using the filament winding process, oriented at  $\pm 55^\circ$ . The morphological parameters for one ply are a fiber volume fraction of 52% and a fiber diameter of 7  $\mu\text{m}$  [15]. The elastic properties of the composite are significantly affected by the orientation, distribution, fraction, and diameter of the fibers. To investigate the impact of these parameters on the elastic properties, we vary each parameter while keeping the others fixed. The table 3 presents the variations of each parameter for this study.

**Table 3.** Variation range of morphological parameters.

<b>Morphological parameters</b>	<b>Variation range</b>	<b>Reference parameters</b>
<b>Fiber fraction</b>	From 30 % to 70 %	52%
<b>Fiber diameter</b>	From 2 $\mu\text{m}$ to 20 $\mu\text{m}$	7 $\mu\text{m}$

The effect of orientation is not considered for this study. In fact, material design give the orthotropic properties of unidirectional composite in the principal coordinate system of ply as shown in table 3 where :

- X : in-plane, in fiber direction
- Y : in-plane, orthogonal to fiber direction
- Z: out of plane, orthogonal to fiber direction

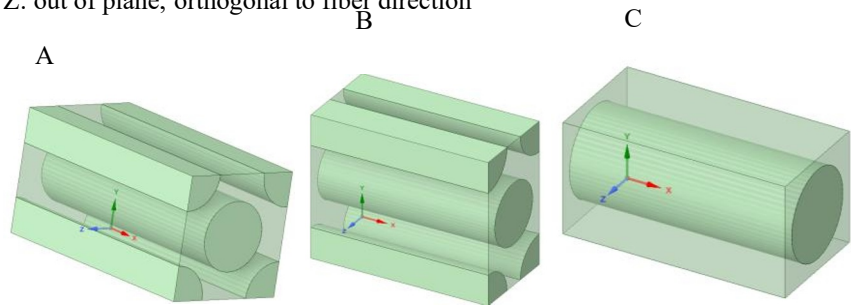


**Fig. 1.** RVE geometries A: Diamond Distribution, B: Hexagonal Distribution, C Square Distribution

## 5 Results and discussion

### 5.1 Effect of unidirectional Glass and carbons Fibers diameters on Young's Modulus:

The results presented in Figure 2 illustrate how fiber diameter influences the elastic modulus of a unidirectional glass fiber/vinyl ester composite and carbon/vinyl ester composite, considering different directions: in-plane fiber direction 1, orthogonal to fiber direction 2, and out-of-plane, orthogonal to fiber direction 3.

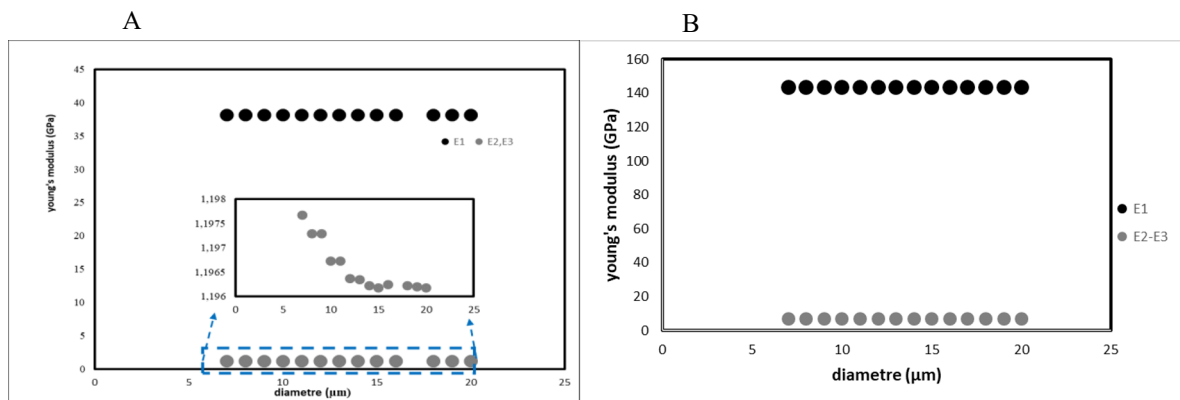


**Fig. 2.** A: variation of Young's Modulus of GFRP with glass fiber diameter,B: variation of Young's Modulus of CFRP with carbon fiber diameter

The behavior of unidirectional materials is orthotropic in both cases: for the isotropic glass fiber and the orthotropic carbon fiber.

The Young's modulus along the fiber direction (E1) and in the orthogonal fiber directions (E2 and E3) remain nearly constant, with E1 around 38 GPa and E2 = E3 approximately 1.97 GPa for the glass/vinyl ester composite, and E1 around 144 GPa and E2 = E3 approximately 7 GPa for the carbon/vinyl ester composite, across the entire range of fiber diameters, from 7  $\mu\text{m}$  to 20  $\mu\text{m}$ .

The minimal variation in all moduli across the fiber diameter range suggests that the in-fiber stiffness of the composite is primarily influenced by factors other than fiber diameter, such as the material properties of the fibers. This behavior is consistent with typical observations in fiber-reinforced composites (reference), where the in-fiber modulus is predominantly determined by the characteristics of the fiber material itself.

## 5.2 Effect of Volume Fraction on Young's Modulus of unidirectional glass fiber

The variation of Young modulus across fiber volume fraction for the unidirectional glass fiber/vinyl ester composite and carbon/vinyl ester composite is presented in the figure 3.

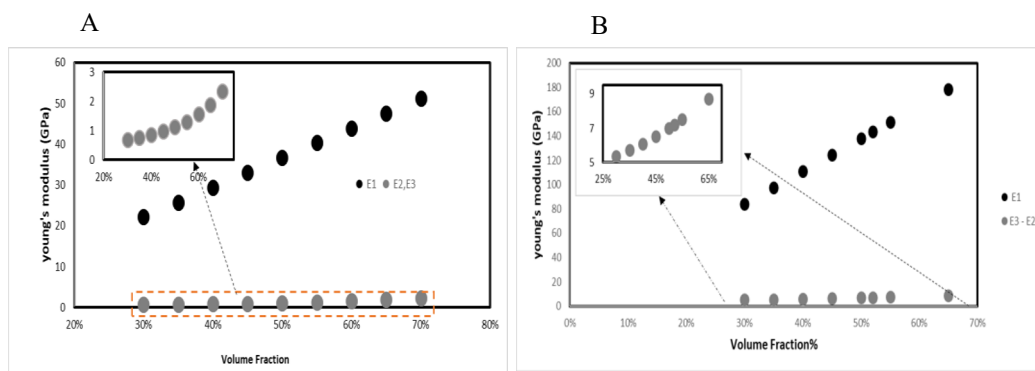


**Fig. 3.** variation of Young's Modulus of : A) GFRP as function of volume fraction of Glass Fiber. B) CFRP as function of volume fraction of carbon Fiber

The in fiber direction Young's modulus (E1) increases significantly as the fiber volume fraction increases. For example, at 30% fiber volume fraction of glass fibers, E1 is 22 GPa, while at 70%, E1 reaches 51 GPa. On the other hand, the orthogonal modulus (E2 and E3) show a more moderate increase as the fiber volume fraction increases. At 30%, E2=E3 is 0.696 GPa, and at 70%, E2=E3 increase to 2.348 GPa.

The modulus E1 increases with fiber content, from 84.28 GPa at 30% fibers of carbon fibers to 178.63 GPa at 65%. This confirms that fibers significantly improve stiffness in the main fiber direction. The difference between the orthogonal modulus, E3-E2, decreases slightly as fiber content decreases, from 8.71 GPa at 65% to 5.37 GPa at 30%, indicating that fibers have a lesser effect on in fiber stiffness.

The results show that stiffness strongly depends on fiber content. The significant increase in modulus (E1) with fiber volume fraction is expected since a higher fiber content in the composite improves its stiffness in the direction of the fibers. The gradual increase in orthogonal moduli (E2 and E3) with higher fiber content suggests that the fiber-matrix interface becomes slightly more efficient at in fiber direction as the fiber volume fraction increases. However, since the matrix phase still has a greater influence in the orthogonal directions, the increase in orthogonal stiffness is less pronounced compared to the in fiber direction. Nevertheless, the rise in E2 and E3 indicates that a higher fiber content improves the composite's performance in orthogonal directions, likely due to enhanced fiber-matrix interactions.

Higher fiber volume fraction improves stiffness, making it ideal for structural applications like pressure pipelines. As fiber content decreases, the matrix plays a bigger role in in fiber stiffness. While adding more fibers enhances axial resistance, it is essential to find a balance since excessive fiber content may reduce impact resistance or increase brittleness.

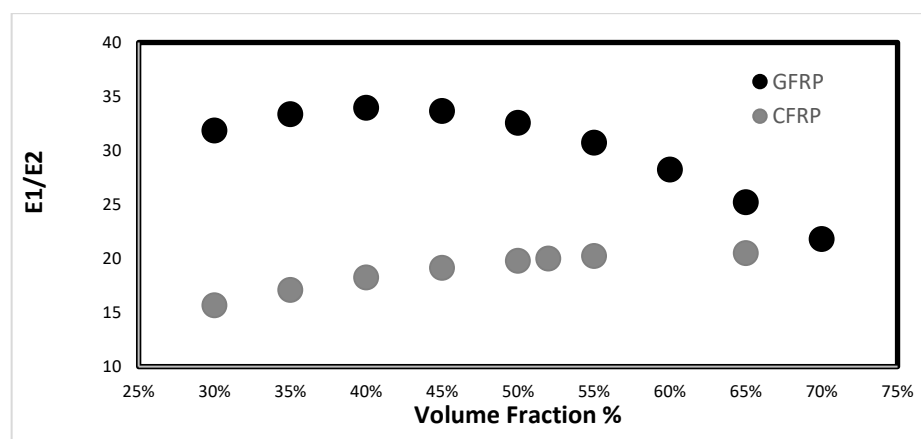


**Fig. 4.** Numerical Evaluation of Anisotropy Ratio E1/E2 for GFRP and CFRP Composites

Figure 4 shows the evolution of the anisotropy ratio E1/E2 as a function of the fiber volume fraction for both GFRP and CFRP composites. The Figure illustrates that for the GFRP composite, the E1/E2 ratio decreases steadily as the fiber volume fraction increases. In contrast, for the CFRP composite, the anisotropy ratio increases significantly with higher fiber content. Throughout the range of fiber volume fractions considered in this study, the CFRP consistently exhibits a higher E1/E2 ratio than the GFRP.

For carbon fibers themselves have an intrinsic ratio of about  $\frac{E_{11}}{E_{22}} = \frac{230}{30} = 10$ , demonstrating strong anisotropy at the fiber scale, the CFRP composite exhibits a greater anisotropy. This suggests that interactions between the carbon fibers and the matrix amplify the difference in stiffness between the fiber and transverse directions in the composite.

In contrast, the GFRP composite, despite being reinforced with glass fibers that are relatively isotropic, still shows a certain degree of anisotropy due to fiber orientation and the fiber volume fraction, this anisotropy in GFRP remains moderate and well controlled, ensuring reliable performance in both the fiber and transverse directions. This balanced behavior makes GFRP a more versatile and robust choice that can be used in pipelines in hydrogen transport applications.

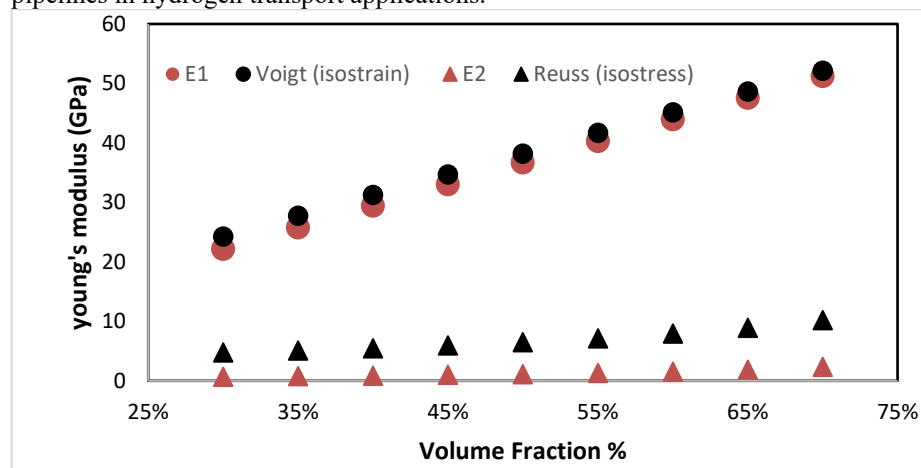


**Fig. 5.** Theoretical Prediction of GFRP Elastic Moduli Using Micromechanical Models

The figure 5 summarizes the theoretical elastic properties of the unidirectional composite estimated using the classical micromechanical model: the Rule of Mixtures that includes the Voigt assumption for isostrain and the Reuss assumption for isostress for GFRP.

## 6 Conclusion

This study highlights the significant influence of morphological parameters on the mechanical performance of unidirectional composite pipelines. Numerical simulations using ANSYS Material Design demonstrated that smaller fiber diameters and higher fiber volume fractions enhance the orthogonal stiffness and overall strength of the composite. Moreover, fiber arrangement patterns play a key role in mechanical response uniformity. When compared to traditional stainless steel pipelines, composite materials, particularly E-glass fiber/vinyl-ester systems, offer promising alternatives for hydrogen gas transport due to their favorable strength-to-weight ratio, corrosion resistance, and adaptability. These findings support the development of more efficient, lightweight, and durable pipeline systems, especially under demanding conditions like hydrogen transportation. Future studies should further explore dynamic loading effects, aging behavior, and real-scale validation to ensure safe deployment in industrial environments.

## References

1. G. Golisch a , G. Genchev , E. Wanzenberg , J. Mentz a , H. Brauer , E. Muthmann , D. Ratke ., « Application of line pipe and hot induction bends in hydrogen gas », *Journal of Pipeline Science and Engineering*, vol. 2, no 3, p. 100067, (2022).
2. E. Mirmahdi, R. Khamedi, D. Afshari, et M. Khosravi, « Investigating the effects of defects and the effect of geometric anisotropy in stainless steel pipes: phased array ultrasonic test, SH-wave », *Journal of Pipeline Science and Engineering*, vol. 3, no 4, p. 100140, 2023.
3. C. Tsiklios, M. Hermesmann, et T. E. Müller, « Hydrogen transport in large-scale transmission pipeline networks: Thermodynamic and environmental assessment of repurposed and new pipeline configurations », *Applied Energy*, vol. 327, p. 120097, (2022).
4. M. Gao, Y. Feng, X. Hu, C.-T. Ng, et A. Kotousov, « Delamination detection in composite pipes using higher harmonic generation of flexural waves », *Composite Structures*, vol. 346, p. 118418, (2024).
5. Z. Li, X. Jiang, H. Hopman, et C. Affolter, « Surface crack growth in metallic pipes reinforced with Fibre-Reinforced Polymers subjected to cyclic loads: An analytical approach », *Theoretical and Applied Fracture Mechanics*, vol. 127, p. 104070, (2023).
6. H. Cai, J. Ye, Y. Wang, Y. Shi, M. Saafi, et J. Ye, « Microscopic failure characteristics and critical length of short glass fiber reinforced composites », *Composites Part B: Engineering*, vol. 266, p. 110973, (2023).
7. M. Abolfazli et al., « Impact of Fire-Retardant coating on the residual compressive strength of hybrid Fibre-Reinforced polymer tubes exposed to elevated temperature », *Composites Part A: Applied Science and Manufacturing*, vol. 193, p. 108831,(2025).
8. Bruno Guilherme Christoff a z, Humberto Brito-Santana, Ramesh Talreja , Volnei Tita “Multiscale embedded models to determine effective mechanical properties of composite materials: Asymptotic Homogenization Method combined to Finite Element Method” *Composites Part C: Open Access* (2022)
9. Shaoyu Zhaoa, Zhan Zhaob, Zhicheng Yangc, LiaoLiang Ked, Sritawat Kitipornchaia, Jie Yangb, “Functionally graded graphene reinforced composite structures: A review” *Engineering Structures*, Volume 210, (2020), 110339
10. R. Nouri, A. Bahlaoui, M. Sammouda, et S. Belhouideg, « COMPORTEMENT MECANIQUE D’UN COMPOSITE VERRE EPOXY UTILISES DANS LES PALES EOLIENNES: COMPARAISON DE MODELES THEORIQUES ».
11. E. Natarajan, L. I. Freitas, M. S. Santhosh, K. Markandan, A. A. Majeed Al-Talib, et C. S. Hassan, « Experimental and numerical analysis on suitability of S-Glass-Carbon fiber reinforced polymer composites for submarine hull », *Defence Technology*, vol. 19, p. 1-11, (2023).
12. J. L. Thomason, « Glass fibre sizing: A review », *Composites Part A: Applied Science and Manufacturing*, vol. 127, p. 105619, (2019).
13. S. Kumar, B. K. Satapathy, et A. Patnaik, « Thermo-mechanical correlations to erosion performance of short glass/carbon fiber reinforced vinyl ester resin hybrid composites », *Computational Materials Science*, vol. 60, p. 250-260, (2012).
14. T. Hasan et al., « Freeze-thaw durability of vacuum infused glass fibre composites with unsaturated polyester and vinyl ester 139037matrices », *Construction and Building Materials*, vol. 455, p., (2024)
15. Zheng Li Tong Li, Bo Wang , Peng Hao, Kaifan Du, Zebei Mao.,«multi-scale numerical calculations for the interphase mechanical properties of carbon fiber reinforced thermoplastic composites », *Composites Science and Technology* (2025).

16. Bruno Guilherme Christoff a z, Humberto Brito-Santana, Ramesh Talreja , Volnei Tita “Multiscale embedded models to determine effective mechanical properties of composite materials: Asymptotic Homogenization Method combined to Finite Element Method” *Composites Part C: Open Access* (2022)
17. K. Bieniek , M. Majewski , P. Hołobut , K. Kowalczyk-Gajewska, “Anisotropic effect of regular particle distribution in elastic–plastic composites: The modified tangent cluster model and numerical homogenization” *International Journal of Engineering Science*(2024)
18. Shaoyu Zhaoa, Zhan Zhaob, Zhicheng Yangc, LiaoLiang Ked, Sritawat Kitipornchaia, Jie Yang “Functionally graded graphene reinforced composite structures: A review” *Engineering Structures* 210(2020)
19. Saiiaf Bin Rayhana, Md Mazedur Rahmanb “Modeling elastic properties of unidirectional composite materials using Ansys Material Designer” *Procedia Structural Integrity* 28 (2020) 1892–1900
20. Eugenio Giner , Ana Vercher , Miguel Marco , Camila Arango “Estimation of the reinforcement factor n for calculating the transverse stiffness E2 with the Halpin–Tsai equations using the finite element method” *Composite Structures* 124 (2015) 402–408